

SPE 16000

Fifth Comparative Solution Project: Evaluation of Miscible Flood Simulators

by J.E. Killough, ARCO Oil & Gas Co., and C.A. Kossack, Norwegian Inst. of Technology

SPE Members

Copyright 1987, Society of Petroleum Engineers

This paper was prepared for presentation at the Ninth SPE Symposium on Reservoir Simulation held in San Antonio, Texas, February 1-4, 1987.

This paper was selected for presentation by an SPE Program Committee following review of information contained in an abstract submitted by the author(s). Contents of the paper, as presented, have not been reviewed by the Society of Petroleum Engineers and are subject to correction by the author(s). The material, as presented, does not necessarily reflect any position of the Society of Petroleum Engineers, its officers, or members. Papers presented at SPE meetings are subject to publication review by Editorial Committees of the Society of Petroleum Engineers. Permission to copy is restricted to an abstract of not more than 300 words. Illustrations may not be copied. The abstract should contain conspicuous acknowledgment of where and by whom the paper is presented. Write Publications Manager, SPE, P. O. Box 833836, Richardson, TX 75083-3836. Telex, 730989 SPEDAL.

ABSTRACT

This paper presents the results of comparisons between both four-component miscible flood simulators and fully compositional reservoir simulation models from seven different participants for a series of three test cases. These cases varied from scenarios dominated by immiscible conditions to scenarios in which minimum miscibility pressure was maintained or exceeded throughout the simulations. In general, agreement between the models was good.

For a test case in which reservoir pressure was maintained above the minimum miscibility pressure, agreement between four-component simulators, with the assumption of complete mixing of solvent and oil, and compositional simulators was excellent based on cumulative oil production as a function of cumulative water injection. For cases in which immiscible conditions dominated, the four-component models tended to be pessimistic compared to fully compositional models because condensable liquids were not considered to be carried in the gaseous phase in the four-component simulations. Relative permeability treatment, especially near the injection well, tended to dominate the timing of recovery and injectant breakthrough.

INTRODUCTION

The simulation of gas or solvent injection into a volatile oil reservoir can be modeled by approximating the phase behavior with four components - oil, water, free/solution gas, and injection gas (solvent)- as described by Todd and Longstaff¹. This process can also be modeled by accurately simulating the phase behavior with n-components whose K-values are complex functions of pressure, temperature, and composition. A precise set of rules of when one may approximate the displacement process with four components and when one must use the fully

compositional formulation is not generally available. There is much discussion in the technical community of exactly this problem, but all too often the decision of which model is used comes from time, money, computer, or data availability or purely subjective reasons. Thus, this comparative solution project has attempted to present an opportunity for the petroleum simulation community to investigate some aspects of this question and at the same time provide an attempt to validate two types of reservoir simulators under certain operating conditions. As was said in the Fourth SPE Comparative Solution Project,² "good agreement between results from different simulators for the same problem does not insure validity of any of the results, (but) a lack of agreement does give cause for some concern."

This paper represents the fifth in a series of comparative solution problems which have been open for participation by oil companies, research institutes, and consultants. The first study was conducted by Odeh³ and consisted of a three-dimensional, two-phase, black-oil simulation. Chappelle and Nolen⁴ organized a study of three-phase, single well radial cross-sectional coning simulations. A compositional, three-phase study of gas cycling in a retrograde gas condensate reservoir comprised the third comparative solution project organized by Kenyon and Behie.⁵ The most recent comparative solution problem conducted by Aziz, Ramesh, and Woo² was a two-dimensional radial steam injection (thermal) simulation.

The object of this paper is to present the simulation problems and selected results as submitted by the participants and to discuss any large differences which exist in the results. Seven participants were involved in this project. An attempt has been made to describe the problems and the input to the simulators in such a fashion that all of the appropriate variables for each participant

References and illustrations at end of Paper.

have been well defined. The hope was then that any differences seen in the simulation results would be caused by differences in the simulators or by differences in the input data that were intentionally left to the discretion of the engineer making the simulation.

Three production/injection scenarios were given for the comparative problem. The discussion of the results for each scenario includes a comparison of results submitted from both four-component and compositional simulations. These comparisons give us a look at the validity of the models for a given scenario. Comparisons of typical four-component results with compositional results show us the differences between the two types of simulators for the various scenarios. A complete set of graphical and tabular results from all of the participants for the three scenarios can be obtained from the authors.

PROBLEM STATEMENT

Three injection and production scenarios were designed to test the abilities of the four-component and compositional models to simulate the WAG (water alternating gas) injection process into a volatile oil reservoir. One reservoir description was used in all simulations. The problem did not necessarily represent a real field application or real fluids. A 7 by 7 by 3 finite difference grid was used as shown in Figure 1. Both the coarse grid and the extremely light reservoir oil were chosen to allow the problem to be simulated in a reasonable amount of computer time with a fully-compositional simulator. The coarseness of the grid produced significant numerical dispersion and/or grid orientation errors for all of the models which were compared. Obviously, for a more realistic simulation, grid refinement or orientation studies might be necessary to better quantify these errors. During the development of the problem, a comparison of results from more finely gridded four-component models was considered; however, for comparisons between the four-component and compositional models it was decided to use a single coarse grid, ignoring numerical dispersion effects.

Each participant was requested to submit simulations of each scenario from a four-component simulator and/or from a compositional simulator. Along with each simulation result, the participant was requested to explain, in a few sentences, which simulator he would choose for each scenario. Since this was an engineering judgement, there is no right or wrong answer to the choice of simulator or the reason for the choice.

The three scenarios involve one WAG injection well located in the grid block with $i=1$, $j=1$, and $k=1$, and one production well located in grid block $i=7$, $j=7$, and $k=3$. The production well is constrained to produce at a maximum oil rate of 12000 STB/D. The minimum bottom hole pressure for the production well was varied among the scenarios. A limiting GOR of 10 MCF/STB and a WOR limit of 5 STB/STB were used for the shut-in criteria for the simulations. The WAG injection schemes and production constraints were altered to give the following properties:

- (1) For scenario one the average reservoir pressure declined rapidly below the initial saturation pressure for most of the simulation.
- (2) For scenario two the average reservoir pressure was maintained well above the original saturation pressure and in the vicinity of the minimum miscibility pressure for the entire simulation.
- (3) For scenario three the average reservoir pressure initially declined below the saturation pressure. Rapid overinjection repressured most of the reservoir to a point near the minimum miscibility pressure.

Figure 2 depicts the typical average reservoir pressure response for the three scenarios. As shown in figure 2, the main difference between scenarios one and three is the rapidity in which average reservoir pressure is raised from natural depletion conditions to minimum miscibility conditions. The minimum miscibility pressure is in the range of 3000 to 3200 psia, depending on the definition used, and the initial saturation pressure for the reservoir oil is 2300 psia. A detailed description of the reservoir and fluid properties and the scenarios is given in the Appendix and in Tables 1-9.

The compositional fluid description was a six component Peng-Robinson (PR) characterization. (See Tables 4 and 5.) All appropriate acentric factors, binary interaction coefficients, and equations coefficients were given. The specification of all equation-of-state parameters eliminated differences in characterization and phase matches in the phase behavior results.

The oil contained the following mole percents: 50% C_1 , 3% C_3 , 7% C_6 , 20% C_{10} , 15% C_{15} , and 5% C_{20} . (See Appendix.) Obviously, these compositions represent an extremely light oil. The injectant gas/solvent contained 77% C_1 , 20% C_3 , and 3% C_6 .

(See Table 5.) The C_6 component was added to the injection gas so the fluid system would reach a critical point and become single phase as might be expected in a condensing gas drive mechanism. Without the C_6 in the gas, this system, in a linear displacement, exhibited the combined condensing/vaporizing mechanism described by Zick.⁶

The four-component fluid description contained details necessary to simulate the three scenarios with a standard four-component, mixing parameter model as described by Todd and Longstaff¹. To generate the "black-oil" PVT properties that correspond with the Peng-Robinson equation-of-state characterization, constant composition expansions and a differential liberation expansion were simulated for both the reservoir fluid (oil) and the injection gas/solvent. In Tables 6 through 8 these results are presented as if they were experimental results from a PVT laboratory. The participants generated the required PVT data for their particular model from these tables. An example of ARCO's four-component model PVT data (Table 9) was included as reference to aid the participants.

In most four-component models there are 3 to 5 parameters or switches which must be set by the user to control the model's calculation of the change from immiscible to miscible conditions. The selection of these parameters affects the ability of the four-component model to emulate the immiscible/miscible process. Participants were required to specify the miscibility parameters for their particular four-component model based on the recovery versus pressure data given in the appendix for the slim tube displacement. (See Figure 3.) A further discussion of these parameters is given in the section on the description of the participants' models.

DESCRIPTION OF THE RESERVOIR SIMULATORS

The following sections describe the reservoir simulators which were used by the participants for the comparative solution project. Most four-component or miscible flood simulators were based on the original work by Todd and Longstaff. The compositional simulation models with the exception of the TDC model used an internal Peng-Robinson equation-of-state for phase equilibria calculations. Further information about the simulators is available from the participants. "Five-point" finite differences were used by all participants.

ARCO

The ARCO miscible flood reservoir simulator is based on a limited-compositional formulation. (See Reference 7.) This formulation allows for the treatment of condensation or vaporization of liquids in gas condensate or volatile oil systems. The model has options for either IMPES or fully-implicit treatment of the finite difference equations. For miscible gas injection situations the Todd-Longstaff mixing parameter formulation is used to account for viscous fingering. For the cases reported here the IMPES technique was employed. Three phase oil relative permeabilities were based on a normalized version of Stone's method I.⁸ For pressures above the "miscibility" pressure, the oil relative permeability from the water-oil two phase data (k_{row}) was used for the solvent and oil phases. Single point upstream weighting of phase transmissibilities was used, although other schemes are available. A preconditioned generalized conjugate residual method was used for the linear equations solution.

The ARCO compositional simulator is a modified version of Scientific-Software-Intercomp's COMP II simulator.⁹ The convergence of the phase equilibria calculations is based on the use of the General Dominant Eigenvalue Method (GDEM) for nonlinear equations.¹⁰ For the comparative solution cases, Stone's method II¹¹ was used for three phase oil relative permeabilities. A maximum trapped gas saturation of twenty percent was used for imbibition gas relative permeabilities. Single point upstream weighting is used for transmissibilities. D4 Gauss was used for all cases for the linear equation solutions.

British Petroleum (BP)

British Petroleum used a modified version of Scientific Software-Intercomp's COMP II reservoir simulator for the solutions. Two modifications which were used included the extended Todd-Longstaff treatment and an associated modification to the relative permeabilities.

For the extended Todd-Longstaff model the hydrocarbon phase existing in each grid block is partitioned into two pseudo-phases, "oil" and "solvent". The pseudo phases are assumed to flow as independent miscible phases with their densities and viscosities given not by their composition, but by the mixing rules proposed by Todd and Longstaff. The saturations of the pseudo phases are found by assuming that the composition of the pseudo oil is known (usually the initial oil composition) and that one of the components acts as a tracer of the pseudo-oil saturation. Any hydrocarbons remaining after the pseudo-oil phase has been subtracted comprise the pseudo-solvent. With two components in a simulation this formulation reduces to precisely the original Todd and Longstaff model.

The parameters for the extended Todd-Longstaff treatment are the mixing parameter ω and the pseudo-oil composition. For the comparative solutions the pseudo-oil composition is assumed to be the initial oil composition and component C20 is used as the tracer.

For the comparative solution cases D4 Gauss and single point upstream weighting of phase transmissibilities were used.

The results from BP were reported for two simulations: standard treatment of compositional phenomena ("BP COMP I") and the extended Todd-Longstaff approach ("BP COMP II").

Computer Modeling Group (CMG)

For the four-component cases Computer Modeling Group's IMEX, four-component, adaptive-implicit, black-oil model was used with the pseudo-miscible option. This option assumes that solvent may dissolve in water but not in the oil phase similar to most of the other four-component-type models in this paper. The Todd-Longstaff mixing parameter approach is used.

The compositional runs were performed using CMG's adaptive-implicit compositional model GEM. A semi-analytical approach was used to decouple the flow equations from the flash equations. A quasi-Newton method (QNSS) was used to solve the resultant flash equations. To insure rapid convergence, the fully coupled well equations were solved simultaneously with flow equations using a Newton Raphson procedure.

Preconditioned generalized conjugate gradients and single point upstream weighting were used for the solutions given in this paper. A modification to Stone's three phase oil relative permeability treatment was used.

Chevron

The Chevron miscible flood simulator ("four-component simulator") is a fully-implicit three-component model based on the concepts outlined

by Todd and Longstaff. As opposed to the other miscible flood models in this paper, the Chevron simulator does not include a free gas component. The Chevron compositional model is a fully-implicit, equation-of-state model. For both miscible flood and compositional simulations, banded gaussian elimination and single point upstream weighted transmissibilities were used. For the miscible flood simulation Stone's method II was used for three phase relative permeabilities; for the compositional simulations a modification to Stone's method was used.

Energy Resource Consultants Limited (ERC)

The simulations by Energy Resource Consultants Limited and Atomic Energy Research Establishment, Winfrith, were performed on a four-component version of the PORES black-oil simulator. PORES has both IMPES and fully-implicit options available. The Todd-Longstaff mixing parameter approach is used for simulation of miscible conditions.

For the comparative solution cases the fully-implicit option was used. Gas relative permeability hysteresis and three phase oil relative permeabilities by Stone's method I were employed.

Reservoir Simulation Research Corp. (RSR)

Reservoir Simulation Research Corp. incorporated an IMPES-type equation-of-state compositional model for the simulations. Single point upstream weighting and red/black line SOR were used in the results presented here. Reference 12 gives further details of this simulator.

Todd, Dietrich, and Chase, Inc. (TDC)

Todd, Dietrich, and Chase used their Multiflood Simulator¹³ for the comparative solution cases. This simulator has been designed to reproduce the effects of major mass transfer and phase transport phenomena known to be associated with the miscible flood process with particular emphasis on CO₂ enhanced oil recovery. For immiscible conditions, phase equilibria may be input to the simulator to represent enhanced oil recovery mechanisms of oil phase swelling with condensed solvent, and vaporization of hydrocarbon fluids into the solvent-rich phase.

Although multiple contact miscible displacement may be represented explicitly with the program through the use of appropriate phase equilibrium data, the philosophy of the program for simulating miscible displacement processes is to maintain segregated solvent-rich and oil-rich regions. The degree of segregation is controlled by a mixing parameter approach to account for viscous fingering phenomenon.

The simulator treats seven components which may partition among three phases: liquid hydrocarbon, gas or solvent rich phase, and aqueous phase. The brine component is confined to the aqueous phase. Five of the six remaining components are allowed to partition between the non-aqueous phases as determined by the input K-values. In addition to pressure, K-values can depend on key component concentrations. One component may partition into the aqueous phase. One of the components is non-volatile, but may

precipitate.

The model uses an IMPES approach enhanced with a stabilized Runge-Kutta time discretization. An implicit saturation option in the x-, y-, and/or z- directions is also available. Two-point upstream weighting of the transmissibilities and D4 Gauss were used for the comparative solutions. K-values were generated as a function of pressure, and C1 and C3 concentrations.

For the fully compositional simulations, the K-values for the five volatile components, and molar volumes for all components were generated using Hagoort and Associates' equation-of-state based program "PVTEE". For the four-component representation, the stock-tank oil and the separator gas are represented by two pseudo components in the normal black-oil fashion except that the solution gas-oil ratios, formation volume factors, densities, and viscosities are represented with K-values, molar densities, mol-weights, z-factors, etc.

Comparison of Model Miscibility Treatments

Several different treatments were used for miscibility conditions in the various Todd-Longstaff formulations presented here. The ARCO model used a single value of the miscibility pressure equal to 3000 psia for the switch to miscibility conditions. (A "ramp" condition was available but not used.) The mixing parameter ω was set to a value of 1.0 corresponding to complete mixing of oil and solvent. CMG also used a mixing parameter equal to 1.0. For CMG, miscibility conditions were allowed to vary with pressure in a linear fashion from completely immiscible conditions at 2300 psia to full miscibility at 3000 psia. Chevron used an ω equal to 0.7 for miscible flood simulations. The Chevron residual oil to solvent flood (SORM4) was varied with pressure according to the following table:

<u>PRESSURE (PSIA)</u>	<u>SORM4</u>
1800.	0.300
2400.	0.230
2800.	0.110
3000.	0.038
3400.	0.000

ERC used a miscibility pressure of 2800 psia. The mixing parameter for ERC was set equal to 0.5 for all runs. The TDC miscible flood simulator used a miscibility pressure linear "ramp" from 1500 to 3200 psia with a mixing parameter of 0.6.

RESULTS

The comparisons of results for the various scenarios are presented in the following sections in three manners. First, the results from the four-component (miscible flood) simulators are compared. Next, compositional model results are examined. Finally, a brief comparison is made between typical four-component and compositional results.

Comparison of Results for Scenario One

As indicated above, scenario one involved a WAG injection case in which the reservoir pressure remained substantially below both the initial saturation pressure and "miscibility" pressure for

almost the entire simulation.

Figure 4 compares the cumulative oil production for all of the four-Component models. Two things are evident from this figure. First, cumulative oil production for the Chevron model is substantially above the results for the other participants. This can be explained by the inability of that model to correctly account for the evolution and production of dissolved gas. The second point is the continued oil production of the CMG model after the other three models have ceased production due to excessive producing gas-oil ratio. An analysis of the GOR and WOR behavior for this case as shown in Figures 5 and 6 gives a clearer indication of the differences in the results. The GOR behavior shown in Figure 5 indicates that the Chevron assumption of ignoring dissolved gas results in a substantially lower GOR for the early time period of the simulation. It is interesting to note that the Chevron results do show gas breakthrough at about the same time as most of the other models. Figure 6 shows that the CMG four-component model had water breakthrough at the producer at about the same time as the other models. The slower increase in both WOR and GOR for the CMG model after breakthrough may result from the use of a different oil relative permeability treatment from the other participants since oil saturation variation with time at the center of the top layer is similar in the different models. (See Figure 7.) As shown in Figure 8 the average reservoir pressures for all of the models were similar with the exception of the Chevron results.

The scenario one compositional simulator results for all participants compared somewhat better than the four-component models. Figure 9 compares cumulative oil production for the compositional models. As shown, the results were quite similar for all participants with deviations of only $\pm 3\%$. The Chevron and RSR models do tend to produce slightly longer than other participants' models before reaching the maximum GOR/WOR limits, although all had comparable total oil recoveries. Figures 10 and 11 show WOR and GOR behavior for the compositional models for scenario one. These figures indicate the reason for the longer production period for the RSR and Chevron models. Although water breakthrough and high GOR production occurred at approximately the same time for all models, both the RSR and Chevron models show a slower rise in both GOR and WOR with time. Again, this may be the result of a different oil relative permeability treatment at the production well for these two models. As shown in Figure 12, average reservoir pressure for all models behaved similarly.

Figures 9-12 also show a comparison of a typical four-component model (ARCO limited-compositional miscible flood simulator) with the compositional models for scenario one. In general, the four-component models tend to be somewhat pessimistic in oil recovery compared to the compositional models due in part to the assumption that the four-component models cannot carry an oil component in the gas phase. Because some oil vaporization did occur in scenario one in the compositional simulations, the four-component GOR behavior is somewhat higher than the compositional models especially after solvent breakthrough. Water breakthrough, high GOR behavior, and average reservoir pressures for both compositional and four-component models tend to be

qualitatively similar.

Comparison of Results for Scenario Two

Scenario two represents a case in which the reservoir pressure was maintained near or above the minimum miscibility conditions.

Figure 13 gives the results for the cumulative oil production versus time for the four-component models in scenario two. As shown in this figure, there is a marked deviation between the TDC model and the other participants. The ARCO and CMG results are similar to one another, and the ERC and Chevron results are higher than the others. These differences in results can be easily resolved. A plot of cumulative oil production versus cumulative water injection as shown in figure 14 shows that the four-component models fall into two groupings. The CMG and ARCO results are still close to one another but higher than the other participants. The differences in results can now be explained in a consistent manner by the value of ω which was used by the participants. Both CMG and ARCO used values of 1.0 for ω in an attempt to obtain a comparison with compositional model results. Chevron, ERC, and TDC used values of 0.6, 0.5, and 0.7, respectively, to show the effect of possible viscous fingering on recovery. The differences in miscibility pressure treatment as described above appears to have a minor effect on results since a higher value of ω for the Chevron model resulted in a slightly lower recovery than predicted by TDC. The TDC model used the highest value of pressure for complete miscibility to occur. This resulted in lower overall recovery. Figures 15 and 16 show GOR and WOR as a function of time. Implicit in this figure is the fact that timing of high WOR and GOR is dependent on the injection volumes. Since both Chevron and ERC injected substantially greater volumes of water at a given time than the other participants, water breakthrough and high GOR behavior occurred earlier in their simulations compared to the others. The average reservoir pressures shown in Figure 17 indicate the effect of the greater volumes of injection for Chevron and ERC resulting in higher pressures for their simulations. As shown in Figure 17 the average pressures for all participants exceeded the minimum miscibility conditions throughout the simulations of scenario two.

The large variation of water injection rate by the participants is probably the result of different gas/solvent relative permeability treatment near the injection well. There are at least two possibilities for injection well permeabilities. First, an "upsteam" relative permeability could be assumed in which all nearwell saturations are assumed to be at 100% of the injected phase saturation or at residual saturations. For the other possibility, a total mobility of phases in the injection grid block could be used. For the total mobility treatment the relative permeability used for the gas/solvent has three possibilities: (1) drainage gas relative permeability, (2) imbibition gas relative permeability, or (3) imbibition k_{row} for gas/solvent, where k_{row} is the oil relative permeability from the water-oil two phase data. Each of these treatments leads to a substantially different injectivity and can cause the major differences in timings for

results as discussed above.

For scenario two the cumulative oil productions versus time for compositional models (Figure 18) showed a substantial deviation for all of the participants. Again, cumulative oil production as a function of cumulative water injection removes most major differences in the results as shown in Figure 19. The deviation of the TDC results from the other participants is probably due to the different treatment of phase behavior in the TDC model compared to the Peng-Robinson equation-of-state models for the other participants. In the TDC model, as described above, the heaviest component is not allowed to volatilize. In addition, K-values are table lookups as a function of pressure and key-component compositions. As shown in Figure 19, the BP model with the extended Todd-Longstaff approach ("BP COMP II") gives somewhat lower recoveries due to the incomplete mixing of "solvent" and "oil" pseudo phases. The standard treatment by BP ("BP COMP I") gave results similar to the other participants.

The marked deviation of the timings of the results is again likely due to the near well treatment of gas/solvent relative permeability. Both the BP and RSR results use drainage gas relative permeabilities for calculation of near-well injectivity. ARCO used a combination of k_{row} and imbibition gas relative permeabilities depending on interfacial tensions, and CMG used k_{row} for the near-injection well conditions. Each of these treatments leads to substantially different injectivities. Figures 20 and 21 show that the GOR and WOR behavior for the scenario two compositional cases. As shown in Figure 22 the average reservoir pressure of the BP, Chevron, and RSR models was somewhat higher due to the larger volumes of water injected. Comparison of oil saturations at center of the top layer (Figure 23) indicates the difference in results caused by the approximate phase behavior treatment in the TDC model.

Figures 18, 20-23 show a comparison of ARCO's four-component results with compositional results for scenario two. The results appear qualitatively similar; the CMG compositional and ARCO four-component results are almost the same. Figure 24 is a plot of cumulative oil production versus cumulative water injection for scenario two for the ARCO and CMG four-component and compositional models. As shown in this figure the results are almost identical. The small deviation that does exist is the result of a slightly smaller volume of solvent injection in the ARCO four-component model. The use of complete mixing ($\omega = 1.0$) in both the ARCO and CMG four-component models does give solutions that are comparable to the compositional results.

Comparison of Results for Scenario Three

Four-component model results for scenario three reflect a behavior similar to the results for scenario one since immiscible conditions dominate the production behavior for this case.

As shown in Figure 25 cumulative oil production for the cases was similar with the exception of the Chevron model. Again, the inability of the Chevron model to handle the production of gas which has evolved from solution causes the major differences in

the results. For the other participants, the length of the simulations differs somewhat due to differences in GOR behavior. Oil production for the CMG case continues longer than any of the other participants. Figures 26 and 27 indicate that the main reason for the differences may be a minor difference in relative permeability treatment at the producer for the CMG case. Both GOR's and WOR's began increasing at the same time for all models except the Chevron model. The WOR climbed somewhat more slowly for the CMG model in turn causing the GOR maximum to be reached well after the other models. As shown in Figure 28, average reservoir pressure showed a somewhat more erratic behavior due to the severity of the injection rates in this case.

Compositional results for scenario three cumulative oil versus time showed a substantial deviation among the participants (See Figure 29.) The plot of cumulative oil production versus cumulative water injection as shown in Figure 30 shows that the results from all participants are comparable. The main difference among the models was the length of time until the GOR limit criterion was met. As shown in Figure 31, GOR's for all models began to climb above 2 MCF/STB at approximately the same time; however, GOR for the CMG and TDC models appeared to rise at a slower rate than the other models. Again, this may be the result of the use of different injectivity treatments. As shown in Figure 32, WOR behavior for all models was similar with breakthrough occurring at about the same time. Average reservoir pressure results for the compositional models were again erratic as shown in Figure 33.

As shown in Figure 31, the main difference in the results for scenario three between the four-component and compositional models is the higher GOR for the four-component models during years 2-8. Again, this is probably the result of the simplistic phase behavior assumptions of the four-component models for this comparative solution project.

Comparison of Simulator Efficiencies

The comparison of simulator efficiencies is based on three criteria reported by the participants: Number of time steps, number of nonlinear (outer) iterations, and CPU time. Since the total number of years to simulate a given case varied widely (especially for scenario two), the length of the simulation should be taken into account when comparing results.

Table 10 compares the CPU time for the different cases. As shown in this table, a variety of computers were used. For the cases which employed the Cray computer, a reasonable comparison of CPU times can be made.

Tables 11 and 12 compare total number of time steps and outer (Newtonian) iterations for each participant for all of the cases. In general, the number of outer Newtonian iterations varied between two to four for each time step for all participants. The lower totals for the number of time steps correspond to fully-implicit treatments while the larger number is more representative of the IMPES models.

These results do not necessarily represent

optimized simulations as far as efficiency is concerned. The emphasis for the comparative solution was on the accuracy of results rather than efficiency.

FOUR-COMPONENT OR COMPOSITIONAL ?

Based on the results given above it is possible to comment on the appropriate model for a given simulation case. The compositional formulation appears to give somewhat more accurate results for the cases in which some of the reservoir oil is volatilized into the gaseous phase (scenarios one and three). The presence of oil in the gas phase results in a more realistic recovery for the compositional case. A four-component model which included some form of volatile component in the gas phase could produce results similar to those for the compositional models; however, this was not investigated in this paper.

The discussion of the previous section indicates that for scenario two, in which minimum miscibility conditions were exceeded during the entire simulation for most grid blocks, four-component results with complete mixing gave excellent agreement with compositional results. If viscous fingering is a dominant mechanism, the use of a Todd-Longstaff approach (or extension) may give more realistic answers in these "miscible" situations.

CONCLUSIONS

The results presented in this paper showed that simulations for scenarios one and three gave comparable results among the various participants for four-component models. For scenario two four-component results show deviations in recovery versus time due to different injection volumes and miscibility parameters for the participants.

Compositional results were similar for all participants for scenario one. For scenarios two and three, differences existed among the compositional results primarily due to differing solvent and water injectivities.

Comparisons of four-component and compositional results showed that for scenario two the models were in good agreement. For the cases dominated by immiscible conditions (scenarios one and three), the four-component models tended to be somewhat pessimistic due to assumptions concerning the phase behavior in the four component models.

These results indicate that for situations in which injection rates are limited by bottomhole pressure constraints, care should be taken in the calculation of near-well phase mobilities and relative permeabilities. Three phase relative permeability treatments near the producer may have affected the results of the four-component models to a lesser extent.

REFERENCES

1. Todd, M. R. and Longstaff, W. J., "The Development, Testing, and Application of a Numerical Simulator for Predicting Miscible Flood Performance", *J. Pet. Tech.*, July, 1972.

2. Aziz, K., Ramesh, B., and Woo, P. T., "Fourth SPE Comparative Solution Project: A Comparison of Steam Injection Simulators", SPE 13510 presented at the Eighth SPE Symposium on Reservoir Simulation, Dallas, 1985.
3. Odeh, A. S., "Comparison of Solutions to a Three-Dimensional Black Oil Reservoir Simulation Problem", *J. Pet. Tech.*, pp 13-25 (January 1981).
4. Chappellear, J. E., and Nolen, J. S., "Second Comparative Solution Project: A Three-Phase Coning Study", Proceedings of the Sixth SPE Symposium on Reservoir Simulation, New Orleans (January 31-February 3, 1982).
5. Kenyon, D. E., and Behie, A., "Third SPE Comparative Solution Project: Gas Cycling of Retrograde Condensate Reservoirs," Proceedings of the Seventh Symposium on Reservoir Simulation, San Francisco (November 15-18, 1983).
6. Zick, A. A., "A Combined Condensing/Vaporizing Mechanism in the Displacement of Oil by Enriched Gases", SPE 15493 presented at the 60th Annual SPE Fall Conference and Exhibition, New Orleans, October 5-8, 1986.
7. Bolling, J. D., "Development and Application of a Limited-Compositional Miscible Flood Simulator", SPE 15998 presented at the Ninth SPE Symposium on Reservoir Simulation, February 1-4, 1987.
8. Stone, H. L. "Probability Model for Estimating Three-Phase Relative Permeability", *Trans. AIME* 249 (1970).
9. Coats, K. H., "An Equation-of-State Compositional Model", SPE 8284, presented at the 54th Annual Fall Conference and Exhibition of SPE, AIME, Las Vegas, Nevada, September 23-26, 1979.
10. Crowe, C. M. and Nishio, M. "Convergence Promotion in the Simulation of Chemical Processes - The General Dominant Eigenvalue Method," *AICHE J.* 21 (1975), 528-533.
11. Stone, H. L., "Estimation of Three-Phase Relative Permeability and Residual Oil Data," *J. Can. Pet. Tech.*, (12), No. 4, pp 53-61 (1973).
12. Young, L. C., "Equation-of-State Compositional Modeling on Vector Processors," SPE 16023 presented at the Ninth SPE Symposium on Reservoir Simulation, New Orleans, February 1-4, 1987.
13. Chase, C. A., and Todd, M. R., "Numerical Simulation of CO₂ Flood Performance," *SPES* December, 1984, 596-605.

ACKNOWLEDGEMENT

The authors would like to express their appreciation to the following participants who provided the data used in this paper:

1. C. S. van den Berghe
British Petroleum Research Centre
Chertsey Road
Sunbury-on-Thames
Middlesex TW16 7LN
England
2. W. Chen
Chevron Oil Field Research Company
P. O. Box 446
La Habra, California 90631

- 3. Yau-Kun Li
Computer Modelling Group
3512 - 33 Street N. W.
Calgary, Alberta T2L 2A6
Canada
- 4. C. D. Fernando
Energy Resource Consultants Limited
15 Welbeck Street
London W1M7PF
England
- 5. L. C. Young
Reservoir Simulation Research Corp.
1553 East Nineteenth Street
Tulsa, Oklahoma 74120
- 6. M. R. Todd
Todd, Dietrich, and Chase, Inc.
16000 Memorial Drive
Suite 220
Houston, Texas 77079

We especially thank Mike Todd for his helpful discussions and comments.

APPENDIX: DESCRIPTION OF THE PROBLEM SIMULATIONS

The three cases used for both the four-component and compositional comparisons were based on the 7 by 7 by 3 finite difference grid shown in Figure 1. The grid and reservoir description are similar to that used in the first comparative reservoir simulation project by Odeh.³ Two wells, one for production and one for injection, were located in opposite corners of the grid. For compositional simulations six components were used for the hydrocarbon fluids. The three cases all involved alternate injection of water and an enriched methane solvent. Tables 1-9 present the details of the model input data.

Scenario One

Oil production at 12000 STB oil per day with a minimum bottomhole pressure of 1000 psia for two years with no injection. At year 2, begin WAG injection with a one year cycle. Maximum Injection Bottomhole Pressure = 10,000 psia, Gas Rate = 12,000 MCF/D, Water Rate = 12000 STB/D.

0.0	to	<2.0 Years	Production only
2.0	to	<3.0 Years	Water Inj. plus Production.
3.0	to	<4.0 Years	Gas Inj. plus Production.
4.0	to	<5.0 Years	Water Inj. plus Production.
5.0	to	<6.0 Years	Gas Inj. plus Production.
6.0	to	<7.0 Years	Water Inj. plus Production.
7.0	to	<8.0 Years	Gas Inj. plus Production.
.....			
.....			

Scenario Two

Oil production at 12000 STB oil per day with a minimum bottomhole pressure of 3000 psia. Begin WAG injection at time 0.0 on a standard three month WAG cycle. Injection Bottomhole Pressure = 4,500 psia maximum, Gas Rate = 20,000 MCF/D, Water Rate = 45,000 STB/D.

0.0	to	<91.25 Days	Water Inj. plus Production.
91.25	to	<182.5 Days	Gas Inj. plus Production.
182.5	to	<273.75 Days	Water Inj. plus Production.
273.75	to	<365.0 Days	Gas Inj. plus Production.
365.0	to	<456.25 Days	Water Inj. plus Production.
456.25	to	<547.5 Days	Gas Inj. plus Production.
.....			
.....			

Scenario Three

Oil production at 12000 STB oil per day with a minimum bottomhole pressure of 1000 psia. Production only for one year, then production plus water injection only for one year. Begin WAG injection at time 2.0 years on a standard three month WAG cycle. Injection Bottomhole Pressure = 4,500 psia maximum, Gas Rate = 30,000 MCF/D, Water Rate = 45,000 STB/D.

0.0	to	<365.0 Days	Production Only
365.0	to	<730.0 Days	Water Inj. plus Production.
730.05	to	<821.25 Days	Water Inj. plus Production.
821.25	to	<912.5 Days	Gas Inj. plus Production.
912.5	to	<1003.75 Days	Water Inj. plus Production.
1003.75	to	<1095.0 Days	Gas Inj. plus Production.
.....			
.....			

TABLE 1
Reservoir Data for the Model Problems

Grid Dimension : 7 x 7 areally with 3 layers
 Water Density (Stock Tank) = 62.4 lb/cuft
 Oil Density (Stock Tank) = 38.53 lb/cuft
 Gas Density (Stock Tank) = 68.64 lb/MCF
 Water Compressibility = $3.3 \times 10^{-6} \text{ psi}^{-1}$
 Rock Compressibility = $5.0 \times 10^{-6} \text{ psi}^{-1}$
 Water Formation Volume Factor = 1.000 RB/STB
 Water Viscosity = 0.70 cp
 Reservoir Temperature = 160 °F
 Separator Conditions (Flash Temperature and Pressure) = $\begin{cases} 60 \text{ °F} \\ 14.7 \text{ psia} \end{cases}$
 Reservoir Oil Saturation Pressure = 2302.3 psia
 Oil Formation Volume Factor = $-21.85 \times 10^{-6} \text{ RB/STB/PSI}$
 Slope Above Bubble Point = 8400.0 ft
 Reference Depth = 8400.0 ft
 Initial Pressure at Reference Depth = 4000.0 psia
 Initial Water Saturation = 0.20
 Initial Oil Saturation = 0.80
 Areal Grid Block Dimensions = 500 ft by 500 ft
 Reservoir Data by Layers (See Table 2)
 No Dip
 Relative Permeability (See Table 3)
 Trapped Gas of 20% Corresponding To Initial Gas Saturation of 65% . (Optional)
 PVT Data (See Tables 4-9 .)
 Wellbore Radius = 0.25 ft
 Well Kh = 10000.0 md/ft
 Well Located in Center of Grid Cells.
 Production Well I=7, J=7, Completed in Layer 3 Only.
 WAG Injector at I=1, J=1, Completed in Layer 1 Only.
 Shut-in Conditions:
 GOR Limit of 10.0 MCF/STB
 WOR Limit of 5.0 MCF/STB
 Maximum Time of Simulation = 20 Years

TABLE 3
Relative Permeability and Capillary Pressure Data

S_w	P_{cow}	k_{rw}	k_{row}
0.2000	45.0	0.0	1.0000
0.2899	19.03	0.0022	0.6769
0.3778	10.07	0.0180	0.4153
0.4667	4.90	0.0607	0.2178
0.5556	1.80	0.1438	0.0835
0.6444	0.50	0.2809	0.0123
0.7000	0.05	0.4089	0.0
0.7333	0.01	0.4855	0.0
0.8222	0.0	0.7709	0.0
0.9111	0.0	1.0000	0.0
1.0000	0.0	1.0000	0.0

Liq.Sat.	P_{cgo}	k_{rlig}	k_{rg}
0.2000	30.000	0.0	1.0000
0.2899	8.000	0.0	0.5600
0.3500	4.000	0.0	0.3900
0.3778	3.000	0.0110	0.3500
0.4667	0.800	0.0370	0.2000
0.5556	0.030	0.0878	0.1000
0.6444	0.001	0.1715	0.0500
0.7333	0.001	0.2963	0.0300
0.8222	0.0	0.4705	0.0100
0.9111	0.0	0.7023	0.0010
0.9500	0.0	0.8800	0.0
1.0000	0.0	1.0000	0.0

Residual Oil to Gas Flood = 0.15
 Critical Gas Saturation = 0.05

TABLE 5
Compositional Fluid Description

Reservoir Fluid Composition (Mole Fractions):

C1 = 0.50
 C3 = 0.03
 C6 = 0.07
 C10 = 0.20
 C15 = 0.15
 C20 = 0.05

Injection Gas/Solvent Composition (Mole Fractions):

C1 = 0.77
 C3 = 0.20
 C6 = 0.03
 C10 = 0.00
 C15 = 0.00
 C20 = 0.00

TABLE 2
Reservoir Data By Layers

Layer	Horizontal Perm.(md)	Vertical Perm.(md)	Porosity (Fraction)	Thickness (feet)
1	500.0	50.0	0.30	20.0
2	50.0	50.0	0.30	30.0
3	200.0	25.0	0.30	50.0

TABLE 2 (Continued)
Reservoir Data By Layers

Layer	Elevation (feet)	Initial P_{oil} (psia)	Initial S_w	Initial S_o
1	8335.	3984.3	0.20	0.80
2	8360.	3990.3	0.20	0.80
3	8400.	4000.0	0.20	0.80

TABLE 4
Peng-Robinson Fluid Description

Component	P_c (psia)	T_c (°R)	MW	Accen.Fac	Critz
C1	667.8	343.0	16.040	0.0130	0.290
C3	616.3	665.7	44.100	0.1524	0.277
C6	436.9	913.4	86.180	0.3007	0.264
C10	304.0	1111.8	142.290	0.4885	0.257
C15	200.0	1270.0	206.000	0.6500	0.245
C20	162.0	1380.0	282.000	0.8500	0.235

For all components: $\eta_A^0 = 0.4572355$
 $\eta_B^0 = 0.0777961$

For single components, the Peng-Robinson parameters A and B are given by:

$$A = \eta_A^0 \frac{P}{P_c} \left[\frac{T}{T_c} \right]^2 \left[1 + k \left(1 - \sqrt{T/T_c} \right) \right]^2$$

$$B = \eta_B^0 \frac{P}{P_c} \frac{T}{T_c}$$

where,

$$k = \begin{cases} [0.37464 + 1.54226\omega - 0.26992\omega^2], & \omega < 0.49 \\ [0.379642 + 1.48503\omega - 0.164423\omega^2 + 0.016666\omega^3], & \omega > 0.49 \end{cases}$$

All binary interaction coefficients are zero EXCEPT:

Between C1 and C15 = 0.05
 C1 and C20 = 0.05
 C3 and C15 = 0.005
 C3 and C20 = 0.005

Fluid densities at separator conditions were obtained using the Peng-Robinson EOS.

TABLE 6
Pressure-Volume Relations at 160°F
(Constant Composition Expansion)

Pressure, psia	Relative Volume	Liquid Saturation
4800.0	0.9613	1.0000
4500.0	0.9649	1.0000
4000.0	0.9715	1.0000
3500.0	0.9788	1.0000
3000.0	0.9869	1.0000
2500.0	0.9960	1.0000
2302.3	1.0000	1.0000
2000.0	1.0668	0.9077
1800.0	1.1262	0.8428
1500.0	1.2508	0.7375
1200.0	1.4473	0.6203
1000.0	1.6509	0.5344
500.0	2.9317	0.2883
14.7	164.0880	0.0000
14.7 @ 60°F	77.5103	0.0100

TABLE 7
DIFFERENTIAL VAPORIZATION OF OIL AT 160°F

Pressure (PSIA)	(1) Oil Relative Volume	(2) Gas Formation Volume Factor	Gas Density (G/CC)	Gas Molecular Weight	Oil Density (G/CC)	Oil Viscosity (CP)	Gas Viscosity (CP)	(3) Solution Gas/Oil Ratio	Dev. Factor Z
4800.	1.2506	1.245	.1115	17.42	.5628	.272	.0170	572.8	.8663
4500.	1.2554	1.216	.1115	17.42	.5607	.265	.0170	572.8	.8663
4000.	1.2639	1.160	.1115	17.42	.5569	.253	.0170	572.8	.8663
3500.	1.2734	1.097	.1115	17.42	.5527	.240	.0170	572.8	.8663
3000.	1.2839	1.015	.1115	17.42	.5482	.227	.0170	572.8	.8663
2500.	1.2958	.9070	.1115	17.42	.5432	.214	.0170	572.8	.8663
2302.3	1.301	.8510	.1115	17.42	.5410	.208	.0170	572.8	.8663
2000.	1.2600	.7352	.0955	17.27	.5490	.224	.0159	479.0	.8712
1800.	1.2350	.6578	.0851	17.20	.5541	.234	.0153	421.5	.8764
1500.	1.1997	.5618	.0698	17.13	.5617	.249	.0145	341.4	.8872
1200.	1.1677	.4266	.0549	17.11	.5690	.264	.0138	267.7	.9016
1000.	1.1478	.3508	.0452	17.13	.5738	.274	.0134	222.6	.9131
500.	1.1017	.1688	.0222	17.49	.5853	.295	.0127	117.6	.9490
14.7	1.0348	.00473	.0011	30.93	.5966	.310	.0107	0	.9947
14.7	1.0000	.00473	.0011	30.93	.6174	.414	.0107	0	.9947

- (1) Barrels of oil at indicated pressure and temperature per barrel of residual oil at 60°F.
- (2) MCP of gas at 14.7 psia and 60°F per 1 RVB of gas at temp and pressure (calculated).
- (3) SCF of gas at temp and pressure per barrel at 14.7 psia and 60°F.

TABLE 8
PRESSURE-VOLUME RELATIONS OF SOLVENT GAS AT 160°F
(CONSTANT COMPOSITION EXPANSION)

Pressure (PSIA)	(1) Relative Volume	(2) Gas Formation Volume Factor	Gas Density (G/CC)	Deviation Factor Z	Gas Viscosity (CP)	Gas Molecular Weight	(3) Volatile Oil in Solvent Gas
4800.	1.000	1.7191	.3072	.8943	.038	23.76	0.
4500.	1.0343	1.6620	.2970	.8672	.037	23.76	0.
4000.	1.1053	1.5551	.2779	.8238	.034	23.76	0.
3500.	1.2021	1.4298	.2555	.7839	.031	23.76	0.
3000.	1.3420	1.2809	.2289	.7501	.027	23.76	0.
2500.	1.5612	1.1007	.1967	.7272	.023	23.76	0.
2302.3	1.6850	1.0201	.1823	.7228	.022	23.76	0.
2000.	1.9412	.8853	.1582	.7233	.019	23.76	0.
1800.	2.1756	.7901	.1412	.7296	.018	23.76	0.
1500.	2.6812	.6413	.1146	.7493	.016	23.76	0.
1200.	3.4969	.4913	.0878	.7818	.014	23.76	0.
1000.	4.3477	.3951	.0706	.8100	.013	23.76	0.
500.	9.6364	.1785	.0319	.8977	.012	23.76	0.
14.7	363.9816	.00448	.0008	.9969	.011	23.76	0.
14.7 @ 60°F	304.5530	.00600	.0010	.9946	.010	23.76	0.

- (1) Volume relative to volume of the original charge at 4800 psia and 160°F.
- (2) MCP of gas at 14.7 psia and 60°F per 1 RVB of gas at temp and pressure (calculated).
- (3) Stock tank barrels of oil per MSCF at 160°F.

TABLE 9
FOUR COMPONENT SOLVENT PVT TABLE
ADDITIONAL PVT TABLE (REPRESSURIZATION DATA)

Pressure (PSIA)	Formation Volume Factor			Solution Gas (MCP/STB)	Viscosity		
	Oil (RB/STB)	Gas (RB/MCF)	Solvent (RB/MCF)		Oil (CP)	Gas (CP)	Solvent (CP)
14.7	1.03480	211.41600	223.21400	0.00000	0.31000	0.01070	0.01100
500.0	1.10170	5.92420	5.60220	0.11760	0.29500	0.01270	0.01200
1000.0	1.14780	2.85060	2.53100	0.22260	0.27400	0.01340	0.01300
1200.0	1.16770	2.34410	2.03540	0.26770	0.26400	0.01380	0.01400
1500.0	1.19970	1.84570	1.55930	0.34140	0.24900	0.01450	0.01400
1800.0	1.23500	1.32020	1.26570	0.42150	0.23400	0.01530	0.01800
2000.0	1.26000	1.13600	1.12860	0.47900	0.22400	0.01590	0.01900
2302.3	1.30100	1.17510	0.98030	0.57280	0.20800	0.01700	0.02200
2500.0	1.32780	1.10250	0.90850	0.63410	0.20000	0.01770	0.02300
3000.0	1.39560	0.98520	0.78070	0.78930	0.18700	0.01950	0.02700
3500.0	1.46340	0.91160	0.69940	0.94440	0.17500	0.02140	0.03100
4000.0	1.53120	0.86210	0.64300	1.09950	0.16700	0.02320	0.03400
4500.0	1.59910	0.82240	0.60170	1.25470	0.15900	0.02500	0.03700
4800.0	1.63980	0.80320	0.58170	1.34780	0.15500	0.02610	0.03800

TABLE 10
Comparison of CPU Times

	Four-Component Models		
	Scenario 1	Scenario 2	Scenario 3
ARCO ¹	7.1	20.1	13.2
Chevron ¹	75.0	186.0	102.0
CMG ²	3062.0	5263.0	4933.0
ERC ³	1191.0	1282.0	1230.0
TDC ⁴	75.0	221.0	298.0

	Compositional Models		
	Scenario 1	Scenario 2	Scenario 3
ARCO ¹	532.1	1045.0	860.5
BP I ¹	500.0	525.0	960.0
BP II ¹	670.0	650.0	890.0
Chevron ¹	740.0	1700.0	1088.0
CMG ²	21177.0	32965.0	33279.0
RSR ¹	17.4	28.7	17.7
TDC ⁴	237.8	344.5	349.0

¹ CRAY X/MP

² HONEYWELL MULTICS DPSS/7

³ NORISK DATA ND 570/CX

⁴ CRAY 1S

TABLE 11
Comparison of Total Number of Time Steps

	Four-Component Models		
	Scenario 1	Scenario 2	Scenario 3
ARCO	372	874	692
Chevron	239	6469	321
CMG	258	553	451
ERC	137	221	118
TDC	237	722	531

	Compositional Models		
	Scenario 1	Scenario 2	Scenario 3
ARCO	641	1473	1075
BP I	914	1293	1684
BP II	900	1356	1224
Chevron	224	479	329
CMG	157	386	304
RSR	898	1182	932
TDC	715	1026	1001

TABLE 12
Comparison of Total Number of Outer Iterations

	Four-Component Models		
	Scenario 1	Scenario 2	Scenario 3
ARCO	742	1748	1407
Chevron	813	2059	1112
CMG	971	1926	1652
ERC	465	888	449
TDC	972	2978	2522

	Compositional Models		
	Scenario 1	Scenario 2	Scenario 3
ARCO	1875	4014	3079
BP I	2183	2955	3893
BP II	2583	3547	2888
Chevron	953	1763	1352
CMG	733	1646	1487
RSR	920	1200	941
TDC	2170	3157	3192

COMPARISON OF AVERAGE RESERVOIR PRESSURES
SCENARIOS ONE, TWO, AND THREE
FOUR COMPONENT MODELS

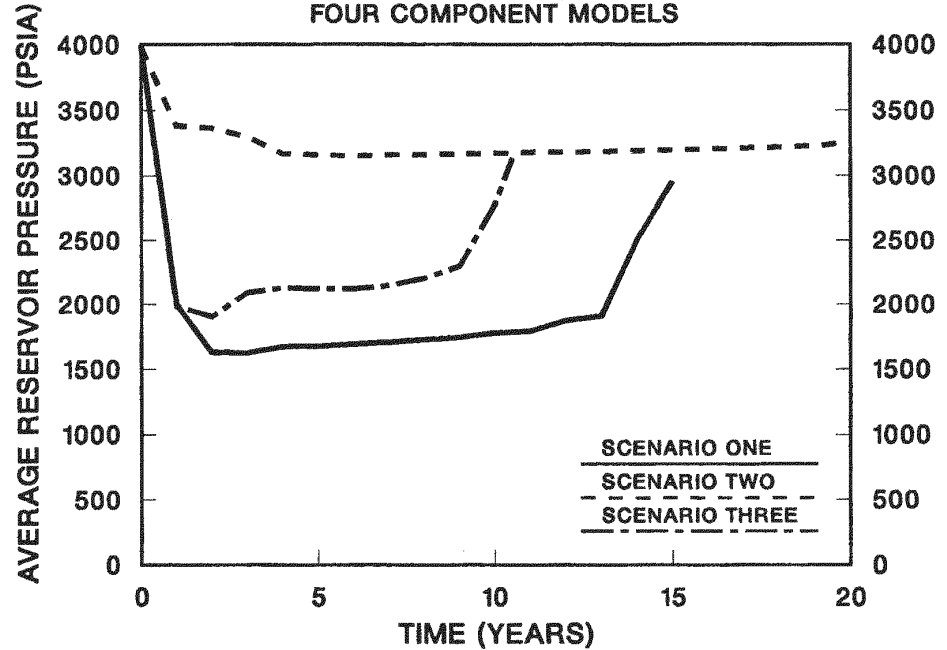


Fig. 2—Comparison of average reservoir pressures for comparative solution Scenarios One, Two, and Three.

GRID FOR COMPARATIVE SOLUTIONS

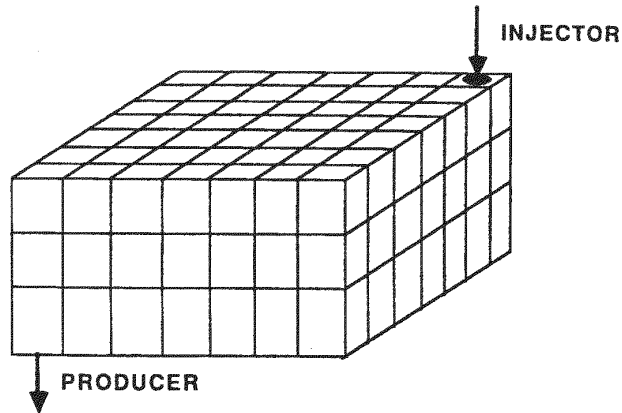


Fig. 1—Three-dimensional finite difference grid for comparative solution problems.

SPE FIFTH COMPARATIVE SOLUTION PROJECT

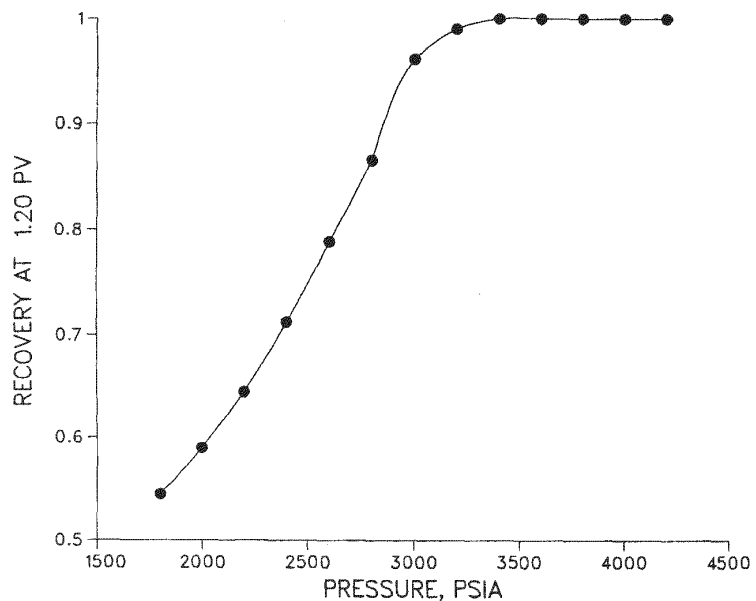


Fig. 3--Stim-tube oil recovery vs. pressure.

COMPARISON OF CUMULATIVE OIL PRODUCTION
SCENARIO ONE
FOUR COMPONENT MODELS

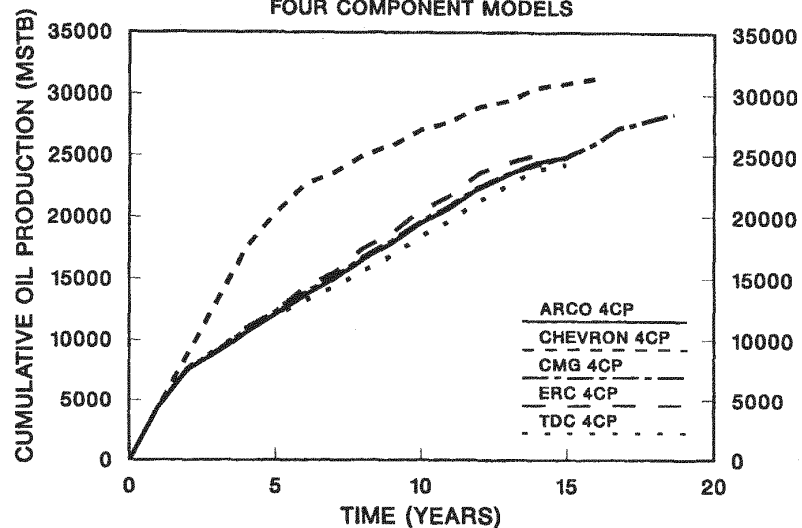


Fig. 4--Scenario One: comparison of cumulative oil production for four-component models.

COMPARISON OF PRODUCING GAS-OIL RATIOS
SCENARIO ONE
FOUR COMPONENT MODELS

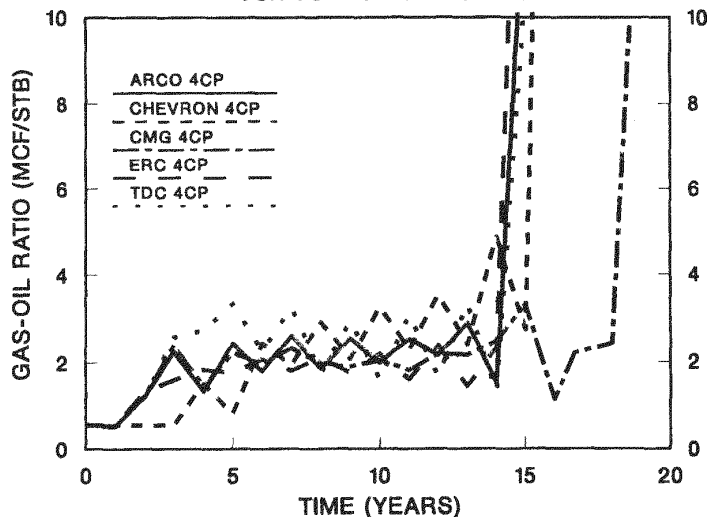


Fig. 5--Scenario One: comparison of producing gas/oil ratios for four-component models.

COMPARISON OF PRODUCING WATER-OIL RATIOS
SCENARIO ONE
FOUR COMPONENT MODELS

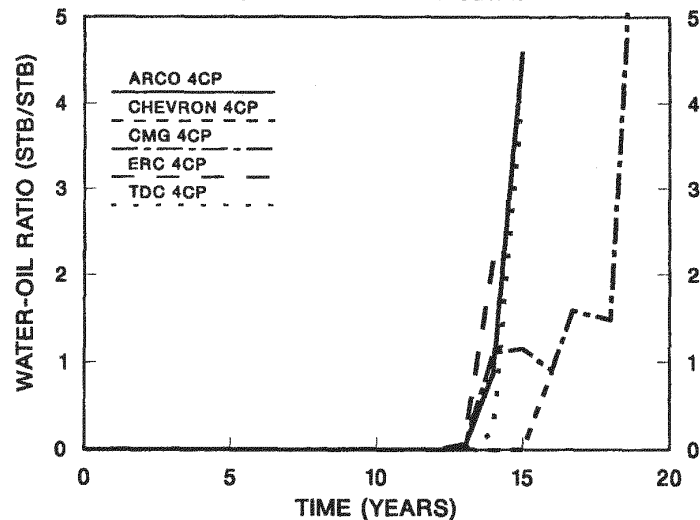


Fig. 6--Scenario One: comparison of producing water/oil ratios for four-component models.

COMPARISON OF OIL SATURATIONS (I=4,J=4,K=1)
SCENARIO ONE
FOUR COMPONENT MODELS

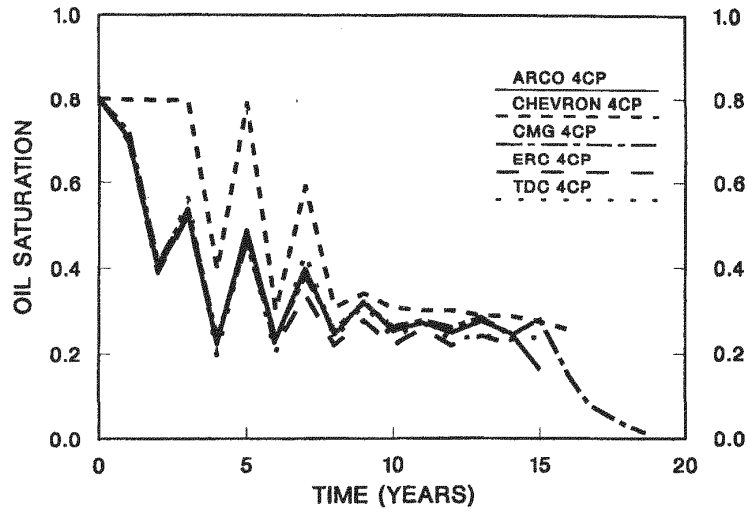


Fig. 7—Scenario One: comparison of oil saturations in location I=4, J=4, K=1, for four-component models.

COMPARISON OF AVERAGE RESERVOIR PRESSURES
SCENARIO ONE
FOUR COMPONENT MODELS

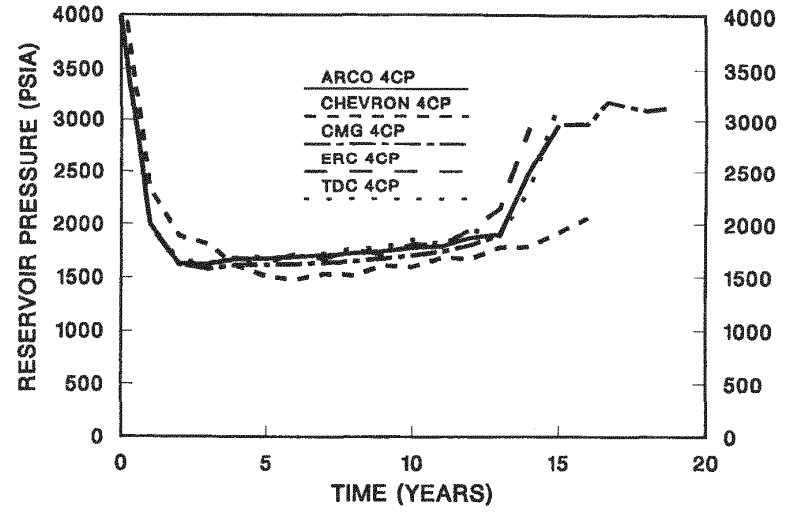


Fig. 8—Scenario One: comparison of average pore-volume weighted pressures for four-component models.

COMPARISON OF CUMULATIVE OIL PRODUCTION
SCENARIO ONE
COMPOSITIONAL MODELS

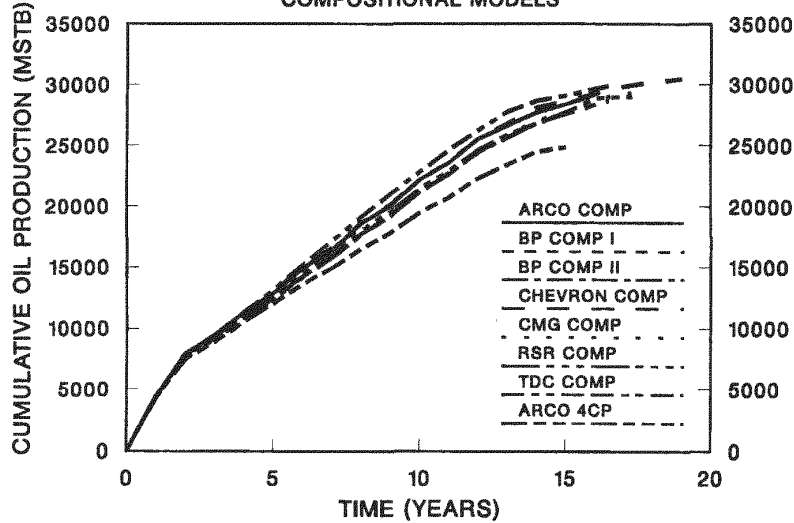


Fig. 9—Scenario One: comparison of cumulative oil production for compositional models.

COMPARISON OF PRODUCING GAS-OIL RATIOS
SCENARIO ONE
COMPOSITIONAL MODELS

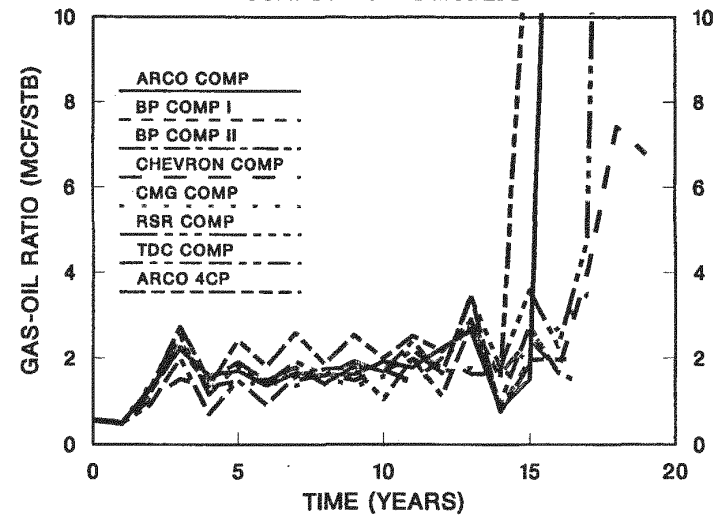


Fig. 10—Scenario One: comparison of producing gas/oil ratios for compositional models.

COMPARISON OF PRODUCING WATER-OIL RATIOS
SCENARIO ONE
COMPOSITIONAL MODELS

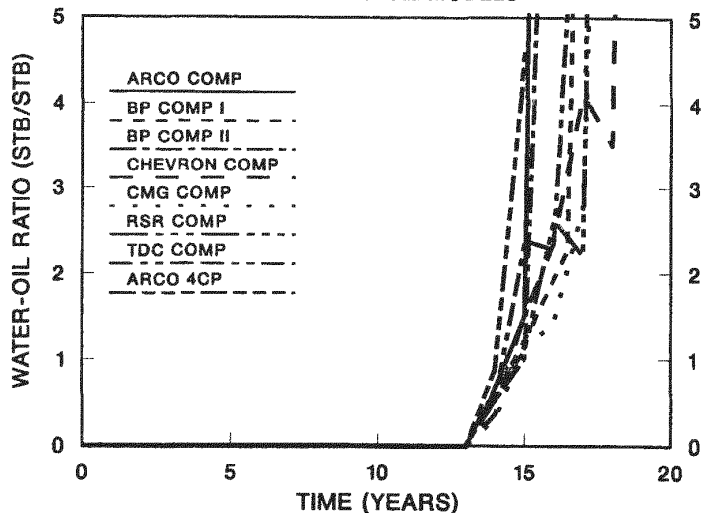


Fig. 11—Scenario One: comparison of producing water/oil ratios for compositional models.

COMPARISON OF AVERAGE RESERVOIR PRESSURES
SCENARIO ONE
COMPOSITIONAL MODELS

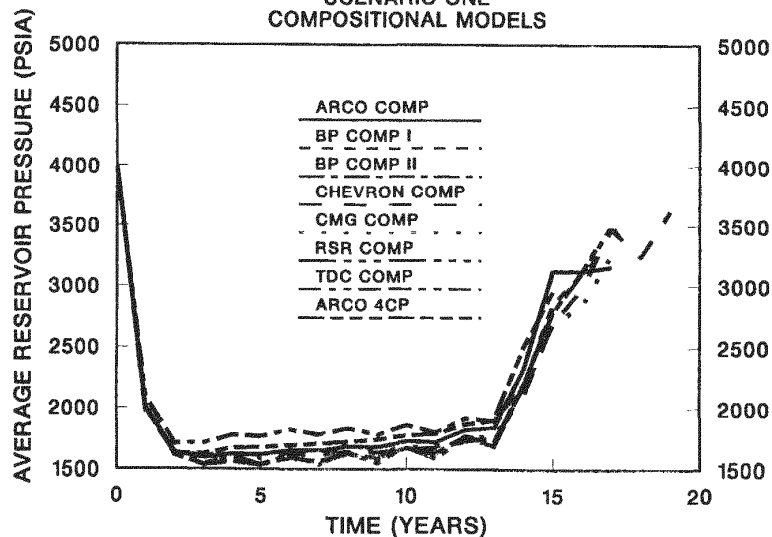


Fig. 12—Scenario One: comparison of average pore-volume weighted pressures for compositional models.

89

COMPARISON OF CUMULATIVE OIL PRODUCTION
SCENARIO TWO
FOUR COMPONENT MODELS

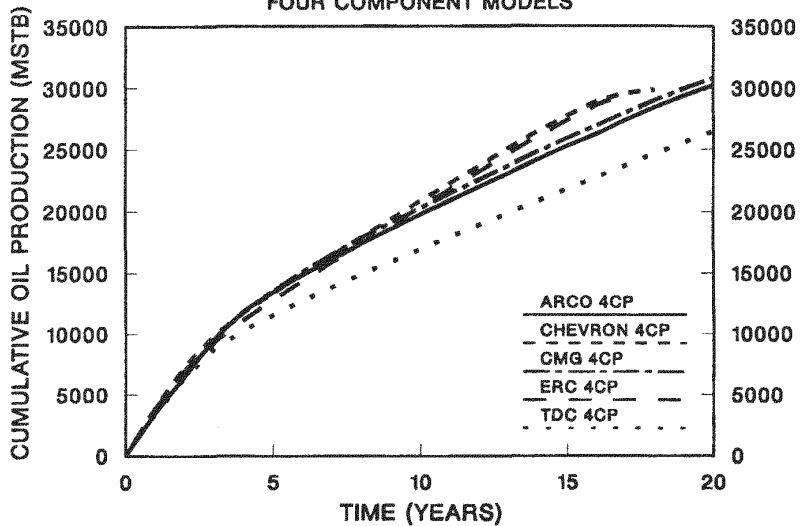


Fig. 13—Scenario Two: comparison of cumulative oil production for four-component models.

COMPARISON OF CUM OIL PROD. VS CUM WATER INJ.
SCENARIO TWO
FOUR COMPONENT MODELS

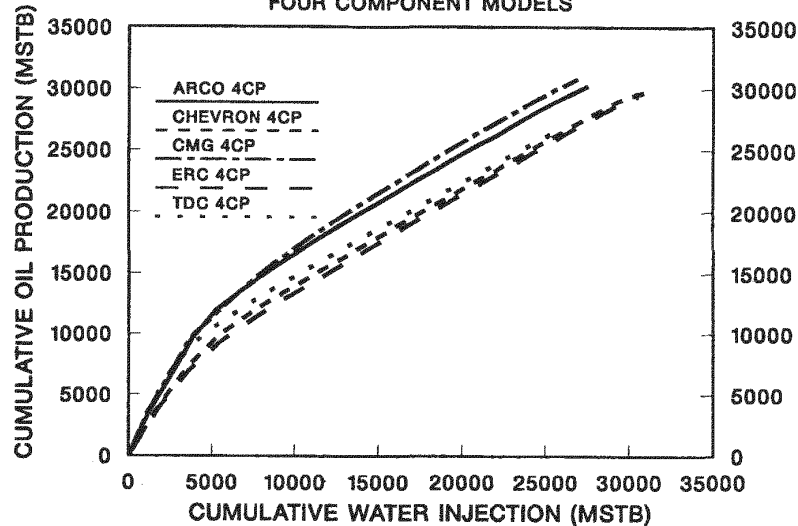


Fig. 14—Scenario Two: comparison of cumulative oil production vs. cumulative water injection for four-component models.

COMPARISON OF PRODUCING GAS-OIL RATIOS
SCENARIO TWO
FOUR COMPONENT MODELS

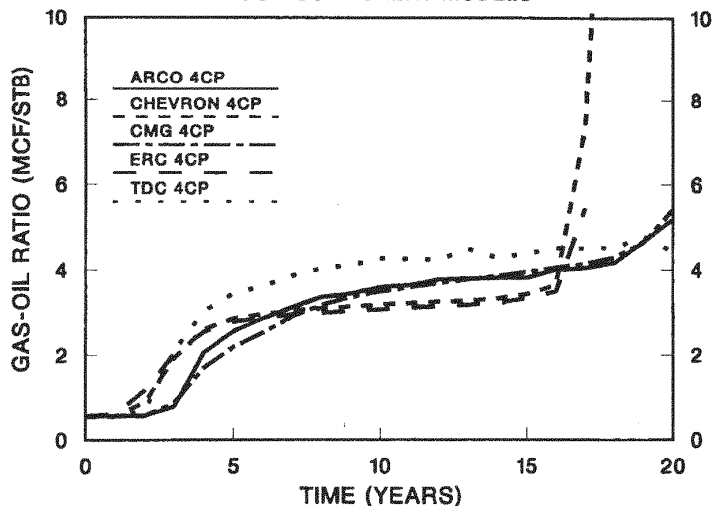


Fig. 15—Scenario Two: comparison of producing gas/oil ratios for four-component models.

COMPARISON OF PRODUCING WATER-OIL RATIOS
SCENARIO TWO
FOUR COMPONENT MODELS

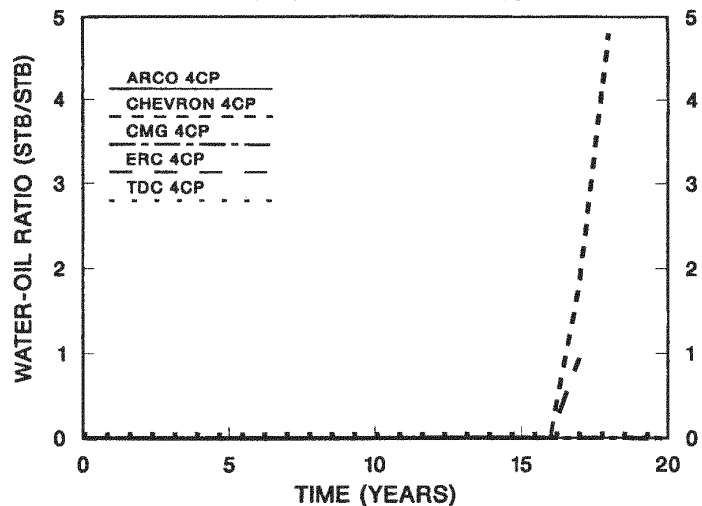


Fig. 16—Scenario Two: comparison of producing water/oil ratios for four-component models.

COMPARISON OF AVERAGE RESERVOIR PRESSURES
SCENARIO TWO
FOUR COMPONENT MODELS

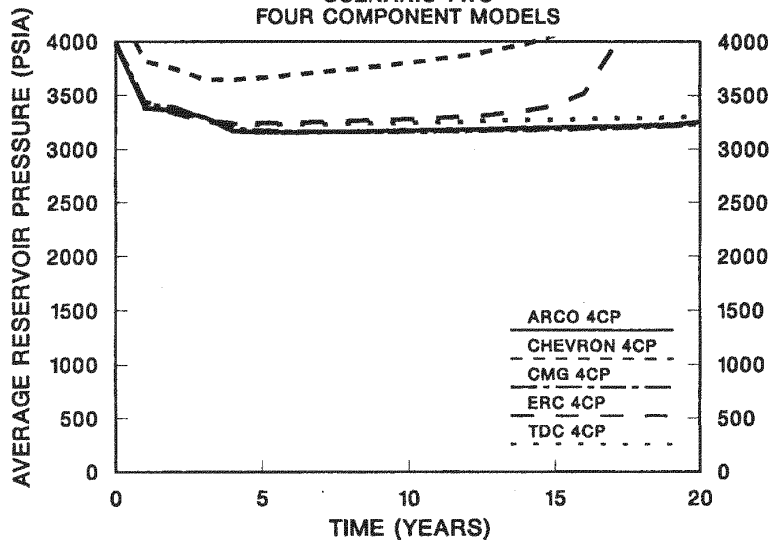


Fig. 17—Scenario Two: comparison of average pore-volume weighted pressures for four-component models.

COMPARISON OF CUMULATIVE OIL PRODUCTION
SCENARIO TWO
COMPOSITIONAL MODELS

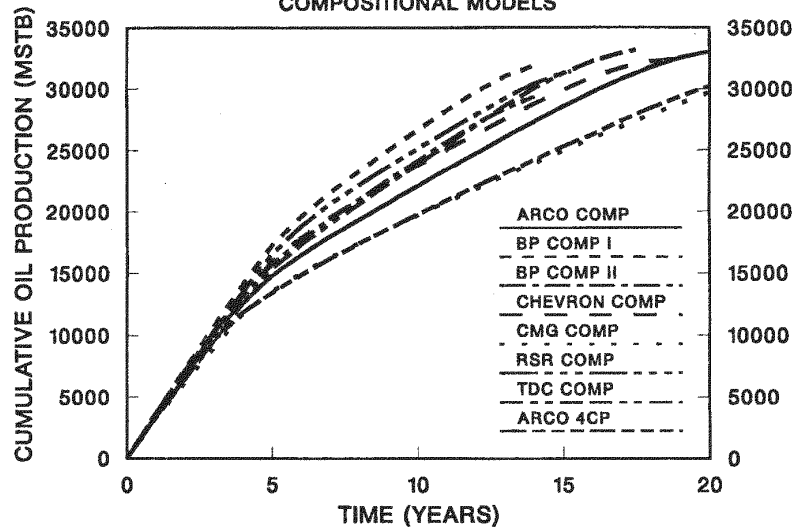


Fig. 18—Scenario Two: comparison of cumulative oil production for compositional models.

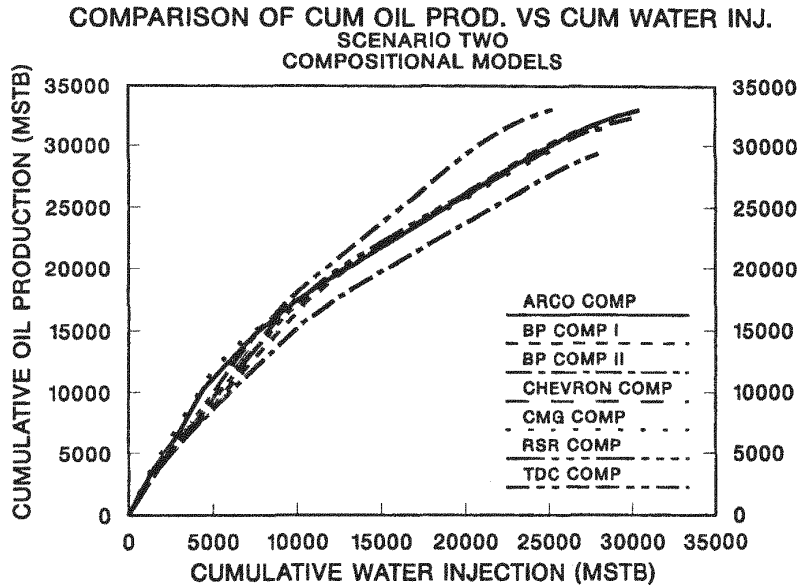


Fig. 19—Scenario Two: comparison of cumulative oil production vs. cumulative water injection for compositional models.

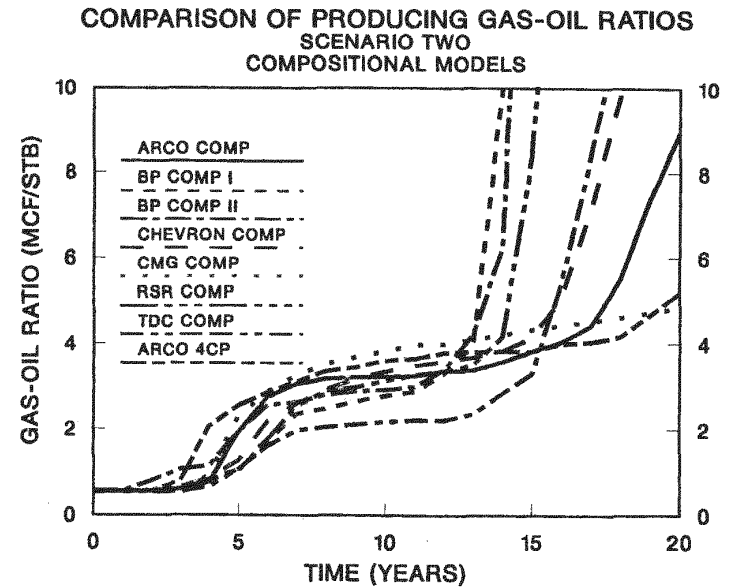


Fig. 20—Scenario Two: comparison of producing gas/oil ratios for compositional models.

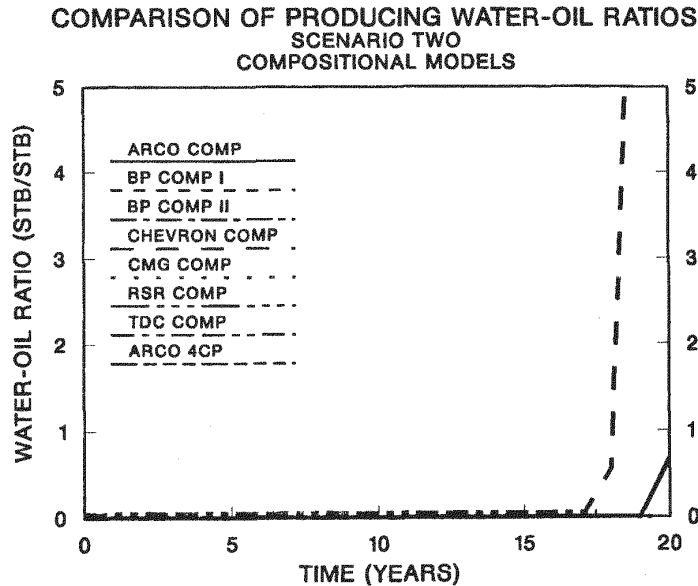


Fig. 21—Scenario Two: comparison of producing water/oil ratios for compositional models.

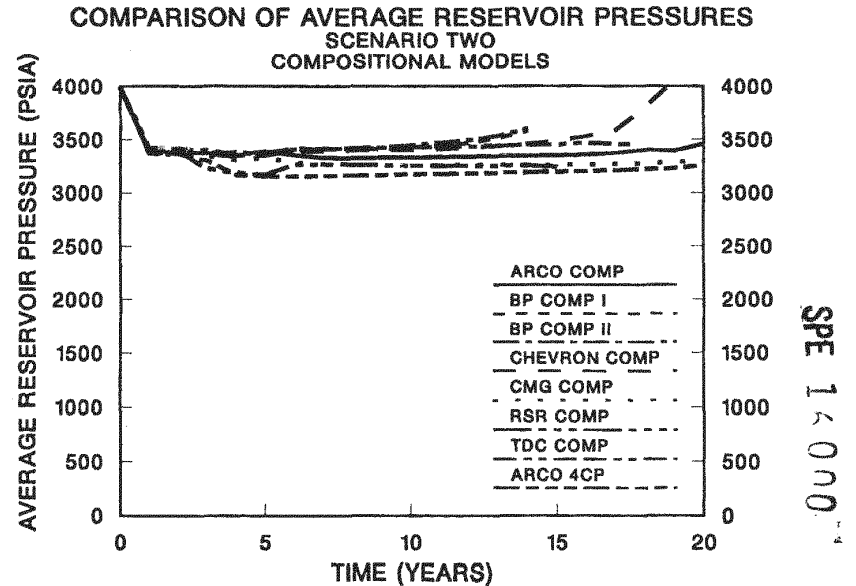


Fig. 22—Scenario Two: comparison of average pore-volume weighted pressures for compositional models.

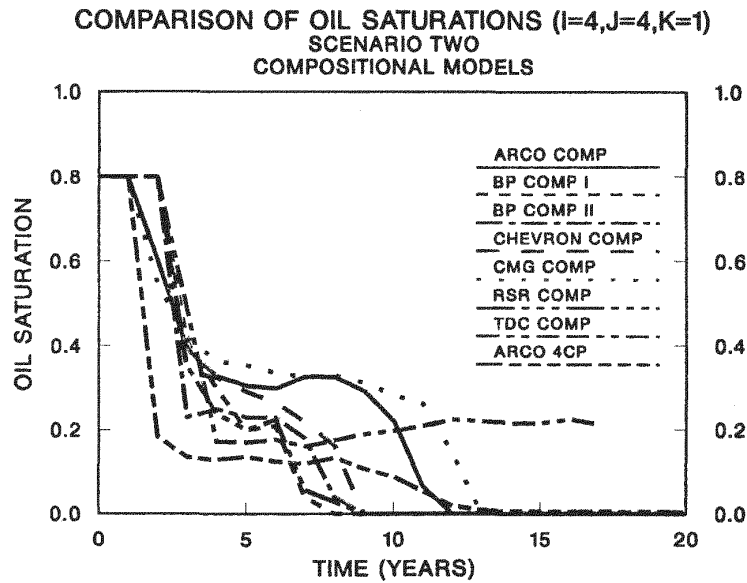


Fig. 23—Scenario Two: comparison of oil saturations in location I=4, J=4, K=1, for compositional models.

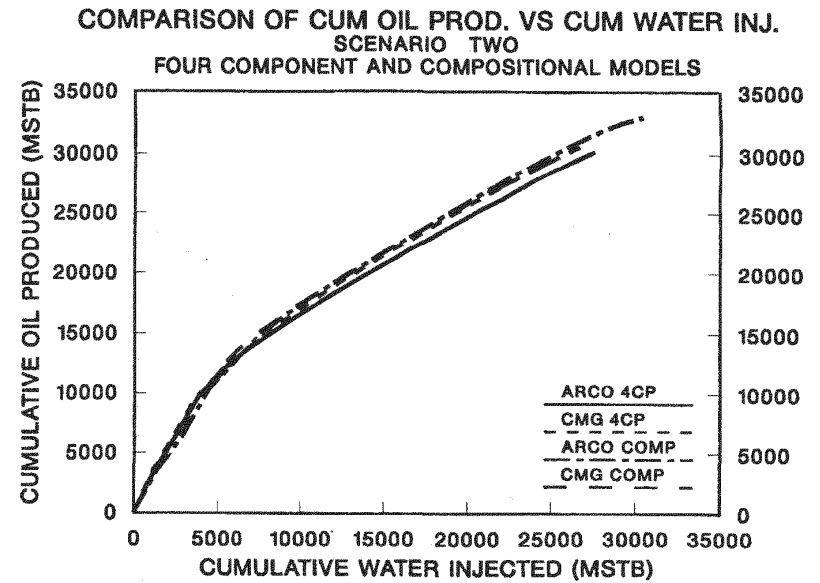


Fig. 24—Comparison of cumulative oil production vs. cumulative water injection for compositional and four-component models (ARCO and CMG).

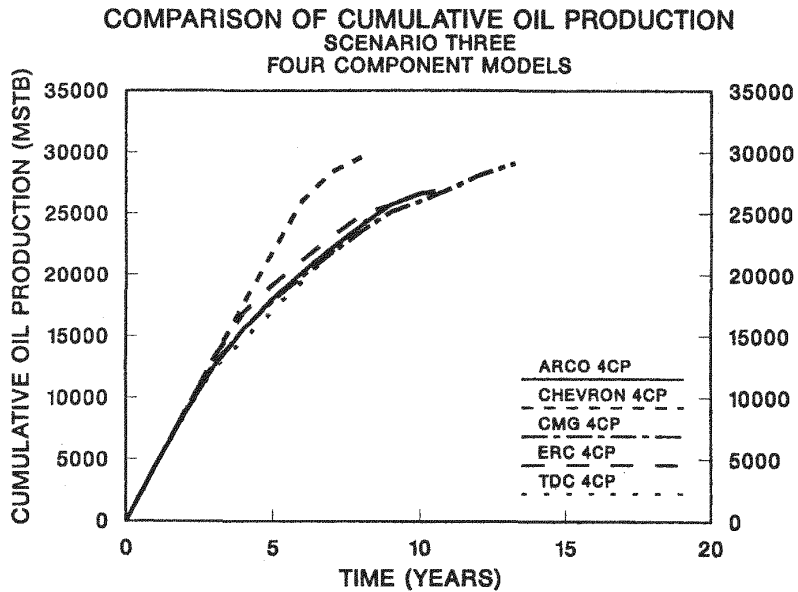


Fig. 25—Scenario Three: comparison of cumulative oil production for four-component models.

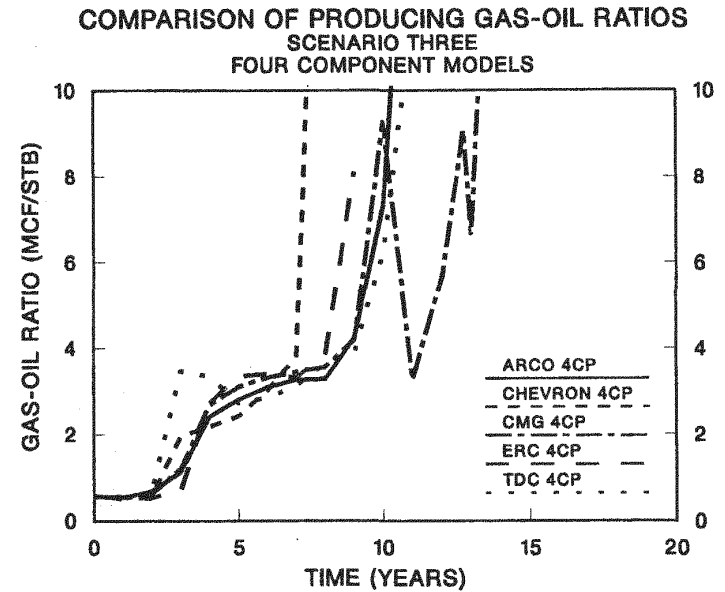


Fig. 26—Scenario Three: comparison of producing gas/oil ratios for four-component models.

COMPARISON OF PRODUCING WATER-OIL RATIOS
SCENARIO THREE
FOUR COMPONENT MODELS

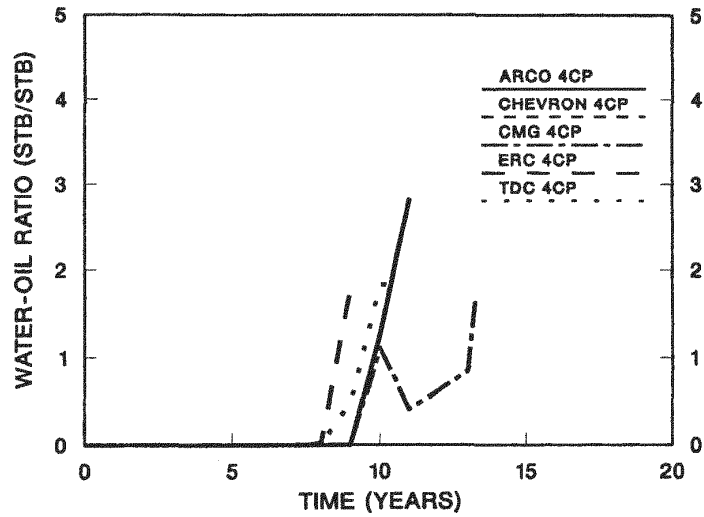


Fig. 27—Scenario Three: comparison of producing water/oil ratios for four-component models.

COMPARISON OF AVERAGE RESERVOIR PRESSURES
SCENARIO THREE
FOUR COMPONENT MODELS

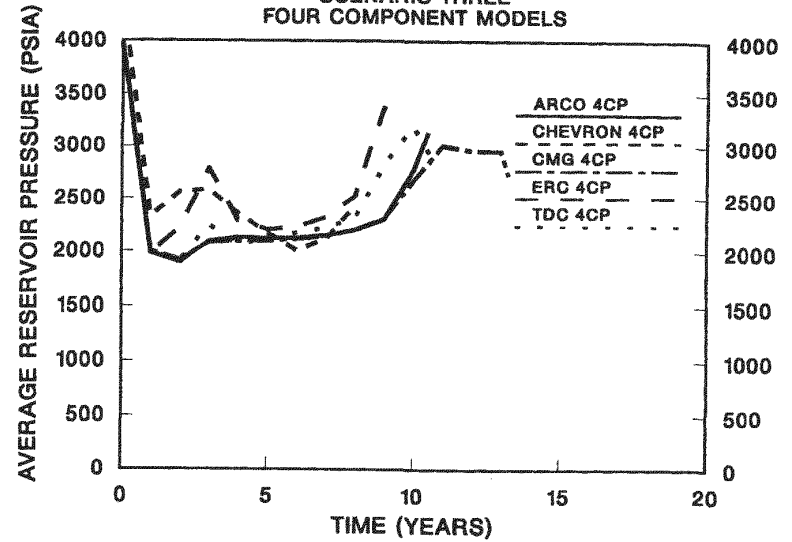


Fig. 28—Scenario Three: comparison of average pore-volume weighted pressures for four-component models.

COMPARISON OF CUMULATIVE OIL PRODUCTION
SCENARIO THREE
COMPOSITIONAL MODELS

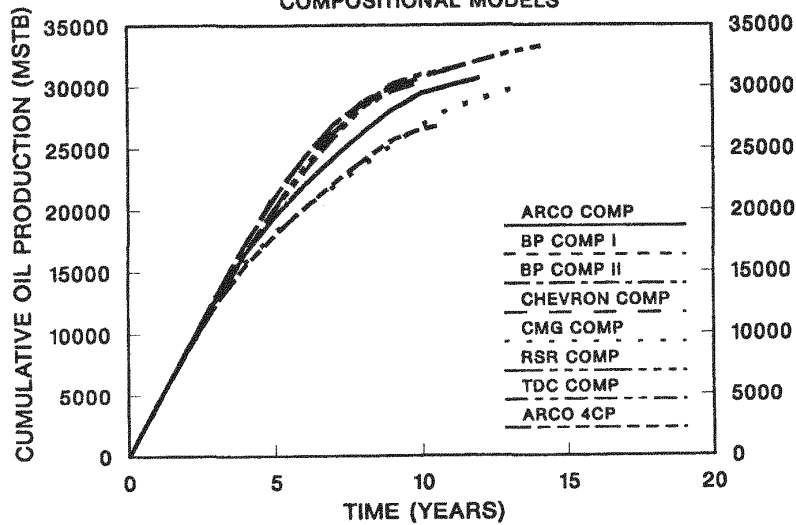


Fig. 29—Scenario Three: comparison of cumulative oil production for compositional models.

COMPARISON OF CUM OIL PROD. VS CUM WATER INJ.
SCENARIO THREE
COMPOSITIONAL MODELS

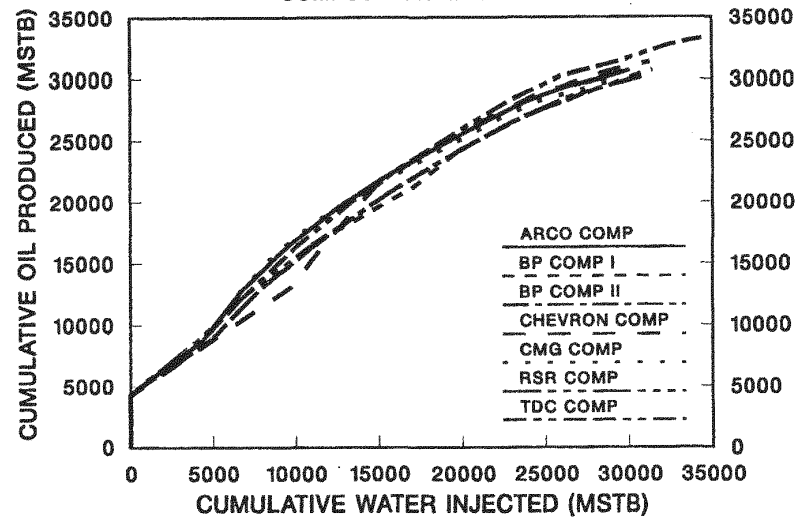


Fig. 30—Scenario Three: comparison of cumulative oil production vs. cumulative water injection for compositional models.

COMPARISON OF PRODUCING GAS-OIL RATIO
SCENARIO THREE
COMPOSITIONAL MODELS

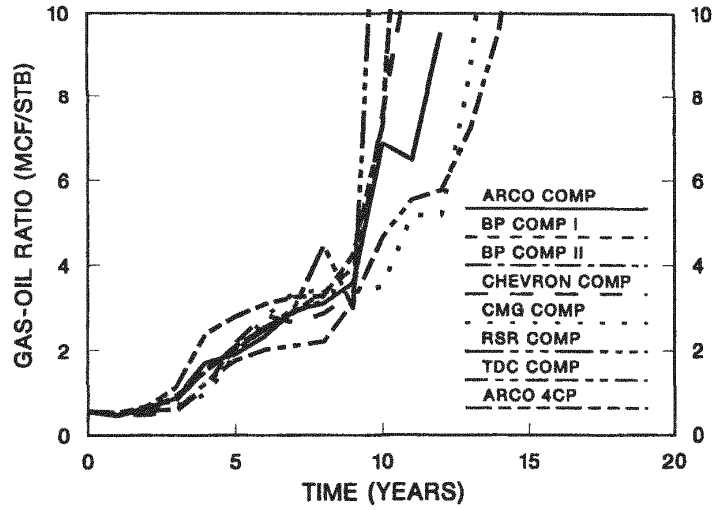


Fig. 31—Scenario Three: comparison of producing gas/oil ratios for compositional models.

COMPARISON OF PRODUCING WATER-OIL RATIOS
SCENARIO THREE
COMPOSITIONAL MODELS

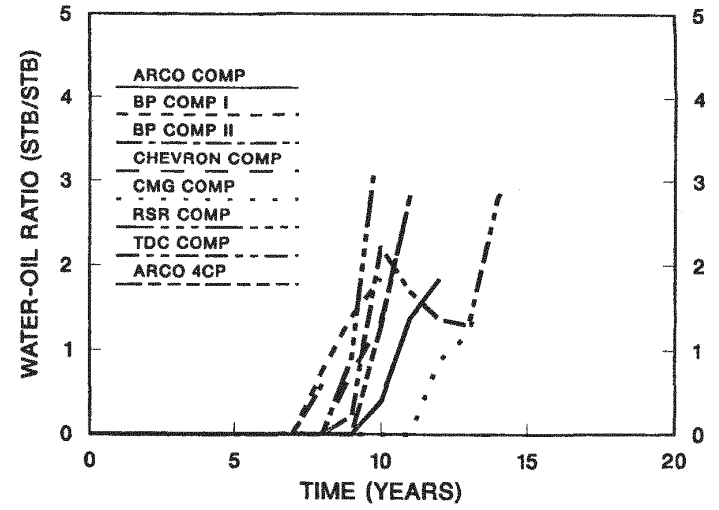


Fig. 32—Scenario Two: comparison of producing water/oil ratios for compositional models.

COMPARISON OF AVERAGE RESERVOIR PRESSURES
SCENARIO THREE
COMPOSITIONAL MODELS

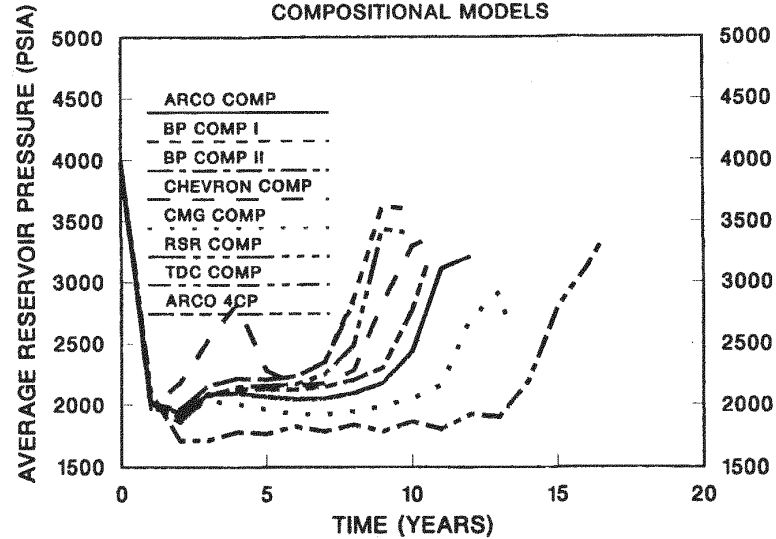


Fig. 33—Scenario Two: comparison of average pore-volume weighted pressures for compositional models.